

Miniature open channel scrubbers for gas collection

Kei Toda ^{1*}, Tomoko Koga ¹, Toshinori Tanaka ¹, Shin-Ichi Ohira ¹, Jordan M. Berg ², Purnendu K. Dasgupta ³

¹ Department of Chemistry, Kumamoto University, Kurokami 2-39-1, Kumamoto 860-8555, Japan

² Department of Mechanical Engineering, Texas Tech University, Lubbock, TX 79409-1021, USA

³ Department of Chemistry and Biochemistry, University of Texas at Arlington, Arlington, TX 76019-0065, USA

* Tel: +81-96-342-3389; Email: todakei@sci.kumamoto-u.ac.jp (K. Toda)

Abstract

An open channel scrubber is proposed as a miniature fieldable gas collector. The device is 100 mm in length, 26 mm in width and 22 mm in thickness. The channel bottom is rendered hydrophilic and liquid flows as a thin layer on the bottom. Air sample flows atop the appropriately chosen flowing liquid film and analyte molecules are absorbed into the liquid. There is no membrane at the air-liquid interface: they contact directly each other. Analyte species collected over a 10 min interval are determined by fluorometric flow analysis or ion chromatography. A calculation algorithm was developed to estimate the collection efficiency *a priori*; experimental and simulated results agreed well. The characteristics of the open channel scrubber are discussed in this paper from both theoretical and experimental points of view. In addition to superior collection efficiencies at relatively high sample air flow rates, this geometry is particularly attractive that there is no change in collection performance due to membrane fouling. We demonstrate field use for analysis of ambient SO₂ near an active volcano. This is basic investigation of membraneless miniature scrubber and is expected to lead development of an excellent micro gas analysis system integrated with a detector for continuous measurements.

Keywords: Planar channel gas scrubber, miniature device for gas collection, theoretical simulation of gas collection, sulfur dioxide, hydrogen sulfide, ammonia

1. Introduction

Miniaturized gas analyzers are of considerable current interest; their application ranges from atmospheric monitoring to medical diagnosis and counterterrorism [1,2]. Often it is not possible for the analysis method to distinguish between gases and particles if both are co-extracted, diffusion based discrimination of gases and particles has emerged to be the method of choice [2-4]. Recently efforts for miniaturization of aerosol collector have been reported such as microbial air sampler [5], miniature cyclones for bioaerosol collection [6], and mixed convection in a narrow rectangular cavity [7]. A micromachined device was also developed for bio-aerosol collection (micro virtual impactor) in which a thick photoresist (SU-8) pattern was fabricated on a 4" silicon wafer and covered with polydimethylsiloxane plate [8]. They succeeded to separate particles at a cutoff size of 1 μm . But few practical approaches to micro gas analyzers have emerged – a well characterized miniature gas collector has been elusive. We have recently demonstrated a honeycomb-microchannel gas scrubber and used it for atmospheric analyses [9,10] and clinical diagnostics [11,12]. Sensitivity and response speeds of the microdevices are predictably much greater than those of conventional collectors such as impingers; the microdevices were possible to continuously monitor ppb-level air pollutants. In the honeycomb scrubbers, the gas phase and absorber solution were separated by a gas permeable membrane that serves to confine the liquid, similar to membrane-based denuders [13]. While a membrane-based construction facilitates liquid containment, mass transfer through the membrane becomes the limiting factor to response speed and often, collection efficiency. If the absorbing solution contains a significant amount of one or more nonvolatile solutes and the sample air is relatively dry, evaporation of the absorber solution at the pores of the membrane results in solid deposits forming in the membrane pores and deteriorates transmembrane mass transfer rates further [14]. Wetted denuders that use no membranes, were reported early on [15,16] and parallel plate geometries appeared thereafter [17]. A miniaturized version of the parallel plate wetted denuder, coupled to a capillary ion chromatograph, was also reported [18]. The fundamental problem with these wetted wall denuders is to achieve proper liquid balance. Because liquid flows down the walls by gravity, the devices must be vertically operated; while the liquid flows down, the air sample is aspirated upwards in a countercurrent fashion. If all the

influent liquid is not fully aspirated out, the excess drops down unto the sampling conduit below and removes soluble gases from the influent sample. On the other hand, if influent liquid flow is too small, dry spots develop on the denuder walls, gas collection efficiency decreases and air is aspirated into the liquid aspiration lines at the bottom that creates problems with some analysis systems. These problems have never been fully solved. An Y-inlet miniature gas collector has been reported by Timmer et al. [19] in which the sample gas and the absorber liquid form alternating segments and the gas bubbles are removed prior to conductivity measurement of the liquid stream. The response time of this device is good but the attainable gas/liquid volumetric ratio is too low for the device to be of general practical interest.

Problems with membrane interfaces between gas and liquid or two liquid phases are also encountered in other areas of endeavor. In gas diffusion flow injection analysis [20], a membrane separates a donor from an acceptor stream and analytes that can be converted to the vapor phase by pH adjustment (e.g., NH_3 , CO_2 , SO_2 , H_2S etc.) or redox transformation (OCl^- , As^{3+} , etc.) are transferred from the donor to the acceptor phase. To allow unmodified samples that can foul a membrane, “pervaporation” arrangements where a headspace exists between the donor stream and the membrane has been advocated [21]. More recently it has also been realized that a membraneless arrangement where the donor and acceptor streams flow side by side may be superior [22,23], following a larger scale earlier demonstration that a wetted denuder can be operated with one wall bearing a donor fluid stream and the opposite wall bearing an acceptor stream [24].

A logical progression of these approaches adapted to gas sampling would be a miniaturized open channel scrubber, can be operated horizontally and will obviate the aforementioned problems with the vertical wetted denuder geometry. We introduce such a device, compare its performance with theoretical simulations, and demonstrate its field use near the Mt. Aso volcanic region.

2. Principles

While the absorber solution is static or flowing along the channel bottom, sample air containing an analyte gas with uniform concentration C_0 is introduced to one end of the channel, as shown in Fig. 1. Absorption of analyte molecules by the liquid surface results in a concentration gradient that drives diffusion from the top of the channel to the gas-liquid interface.

Species transport in laminar flow through narrow ducts may be decomposed as pure convection along the flow direction and pure diffusion normal to the flow direction. Gormley [25] and Gormley and Kennedy [26] described transport of a single species in a narrow rectangular channel and thin circular tube, respectively, and provided approximate numerical solutions. For a channel length direction coordinate x , height direction coordinate y , the transport of analyte in a rectangular channel is modeled thus [25]:

$$D \left(\frac{\partial^2 C}{\partial y^2} + \frac{\partial^2}{\partial z^2} \right) - \frac{\partial}{\partial x} (uC) = 0 \quad \dots (1)$$

where u (m s^{-1}) is the flow velocity in the x direction, C is the gas concentration at any point, and D ($\text{m}^2 \text{s}^{-1}$) is the diffusion coefficient of the analyte in air. If the channel is much wider than it is high and the side walls are chemically inert, then it can be further assumed that all flow and species properties are uniform in the cross-channel direction, z . Then (1) becomes:

$$D \frac{\partial^2 C}{\partial y^2} - \frac{\partial}{\partial x} (uC) = 0 \quad \dots (2)$$

The no-slip condition implies zero air velocity at the channel walls and continuity of velocity across the gas-liquid interface. When the gas velocity is substantially greater than the liquid velocity, this interface velocity may be approximated as zero. With the additional assumptions that the laminar flow is fully developed, the gas velocity depends on y and has the parabolic form,

$$u(y) = \frac{6Q}{HW} \frac{y}{H} \left(1 - \frac{y}{H} \right) \quad \dots (3)$$

where Q ($\text{m}^3 \text{s}^{-1}$) is the volume flow rate and W (m) is the channel width. Denuder models based on eq. 3 may underestimate species removal in the entry region of the channel, before the

parabolic flow profile is fully established.

Gormley [25] treats only the case where both the top and bottom bounding surfaces are perfect sinks for the analyte. More accurate numerical solutions for this case, as well as consideration of the present case where only one surface is a sink are reported by McCuen [27] and Lundberg et al. [28]. Lundberg et al. also provide solutions for annular flow with a variety of geometries and boundary conditions. While these calculations were intended for heat transfer problems, they apply equally well to mass transfer problems. For the uninitiated, however, the use of the original tables from Lundberg et al. is difficult; solutions directly relevant to the annular denuder geometry have recently been made available in spreadsheet form [29]. We similarly use here a spreadsheet implementation of the solutions for the planar geometry; the spreadsheet included in supporting information (PlanarDenuderEfficiencyCalculator.xls).

3. Experimental

3.1. Planar open channel scrubber

Structure of the planar open channel scrubber is shown in Fig. 2. The device constitutes of a gas channel plate and a solution channel plate both made of transparent polyvinylchloride (PVC) that lie above each other, each bearing a 4 mm wide channel. The length and the depth of the liquid channel were 60 and 0.5 mm, respectively. The gas channel made on the top PVC plate extended 10 mm beyond the length of the liquid channel at each end (to allow laminar flow to develop prior to liquid contact), thus totaling 80 mm and to accommodate the substantially greater gas flow rate, the gas channel depth was made 1.5 mm, except as stated. The exterior total dimensions of each plate was 26 mm in width and 100 mm in length. Total height of the device was 22 mm when 1.5 mm deep air channel was used. The bottom of the liquid flow channel was made hydrophilic by placing a thin (100 μm) cotton mesh. Thin filter paper was also found to work but since analyte retention is a possibility, it was not used. We also carried out some experiments by coating with liquid glass (sodium silicate, Nacalai Tesque, Kyoto, Japan) and baking but over a period of time the layer dissolves. For comparison purposes, we

also carried out experiments where a thin porous membrane was placed between the top and bottom plates to provide more conventional membrane-based scrubber. Porous polytetrafluoroethylene (pPTFE), (30 μm thick, pore size 0.45 μm , Poreflon[®] HP-010-30, Sumitomo Fine Polymer, Osaka, Japan), porous polypropylene. (pPP), (94 μm thick, Accurel[®] PP 1E, Membrana, Wuppertal, Germany) and silicone (50 μm thick, Asone, Tokyo, Japan) were each tested.

3.2. Procedure

The sample gas was aspirated through the scrubber device at 25 – 500 mL min^{-1} by a diaphragm airpump, DA-5S (ULVAC Kiko, Saito, Japan) with flow rate control by a mass flow controller (MFC), SEC-B40 (500 mL air/min full scale, Horiba STEC, Kyoto, Japan) and with a liquid mist trap before the flow controller. The absorbing solution was pumped (50 $\mu\text{L min}^{-1}$) into the liquid channel by a peristaltic pump (Minipuls 3, Gilson International) with 0.25-mm i.d. PVC pump tube (15.0 rpm) and aspirated from the liquid outlet at a higher aspiration rate (~ 100 $\mu\text{L/min}$, 0.38 mm i.d. pump tube); some air is obligatorily aspirated but the entire channel remains wet. The pump transfers the aspirated solution into a 10 mL volumetric flask. After 1.0 L of air is sampled, the liquid and air flows are stopped and the liquid volume is made up to 10 mL with distilled deionized water. The respective absorbing solutions were 0.1 M NaOH with 0.02% w/v ascorbic acid for the measurement of H_2S , 0.03% H_2O_2 + 10 μM H_3PO_4 for SO_2 and 5 mM H_2SO_4 for NH_3 . For H_2S and NH_3 , the collected absorber solution was measured by flow injection analysis (FIA), respectively using 5- μM fluorescein mercuric acetate (FMA) in 0.1 M NaOH [30] and 2-mM *o*-phthalaldehyde (OPA) + 3-mM Na_2SO_3 (pH 11 adjusted with $\text{Na}_2\text{B}_4\text{O}_7$ + NaOH) [31]. The carrier and reagent streams flowed at 0.15 mL min^{-1} , respectively, and 100 μL of the collected absorber (after make-up to 10 mL) was injected into the carrier stream. Sulfur dioxide was measured as SO_4^{2-} by ion chromatography under chromatographic conditions previously described [32].

3.3. Field application

In order to evaluate this method, the system was put in a plastic box (35 cm x 29 cm x 17 cm)

including an air pump (DA-5S, ULVAC Kiko) and a small peristaltic liquid pump (high performance roller pump, Ogawa Shokai, Kobe, Japan) with PharMed[®] tubing (0.5 mm i.d. x 3.7 mm o.d. for introduction and 1.0 mm i.d. x 3.0 mm o.d. for aspiration, at 5 rpm) and MFC setup. The entire package was 6.2 kg (5.0 kg without air pump) in weight. The system was much lighter than the commercial pulsed UV fluorescence instrument (APSA-370, Horiba, Kyoto, Japan) used for concurrently measuring atmospheric SO₂ (19 kg). For the scrubber, air was sampled through a dust filter (Balston DFU[®] model 9900-05, Grade BK, Parker) at a flow rate of 100 mL min⁻¹. Gaseous SO₂ absorber and absorber flow rate were the same as in-lab experiments. The effluent absorber was collected into 1.5-mL vials, changed every 10 min. The collected samples were analyzed by ion chromatography upon return to the laboratory on the same day. The instruments were powered by a generator (EU-9i entry, Honda, Japan) placed 20 m downwind from the samplers.

4. Results and discussion

4.1. Membraneless device collection efficiency

Collection efficiencies (f) for NH₃, H₂S and SO₂ are shown in Fig. 3, the respective diffusion coefficients (D) being 0.240, 0.184 and 0.142 cm² s⁻¹, respectively, at 298K and 1.00 atm obtained by Fujita's equation [33,34]. Molecular weights of these gases range from 17 to 64. Lighter molecules predictably have a higher D and result in higher f values. As shown in Fig. 3, the experimental values for the three gases agreed quite well with the theoretical estimates. This provides confidence that collection efficiencies for such devices can be estimated very well *a priori*.

Figure 4 shows variation of f against gas flow rate obtained for H₂S for three different channel depths. The residence time of the sample gas in the scrubber was proportional to the channel depth but a greater counteracting effect was increased mean diffusion distance to the absorber surface. The net result was that a smaller channel depth was the most advantageous, as correctly predicted by theory. At higher gas flow rates and larger channel depths, the observed collection efficiencies were significantly greater than those theoretically predicted.

We used a gas inlet perpendicular to the channel (Fig. 2); with larger channel depths and higher flow rates, laminar flow was not fully developed – for a simple tube the inlet length L_i needed for laminar flow development is approximately (98% accuracy) given by [35]:

$$L_i = 0.2 Q\rho / (\pi\eta) \quad \dots(3)$$

Where Q is the volumetric sampling rate, ρ is the sample gas density and η is its viscosity. The need for a greater inlet length thus directly increases with the sampling rate.

4.2. Comparison with membrane-based scrubbers

In all membrane-based collectors, mass transport through the membranes is generally the factor that limits how much of the sample gas is collected. The results are presented in Fig. 5. With silicone membrane, f was only 7.7% even at 25 mL min⁻¹ and decreased to 0.25% at 500 mL min⁻¹. The pPTFE membrane was the best among the tested membranes. However, the observed collection efficiency was less than that of the membraneless/theoretical case throughout the flow rate range, ranging from 87% of the membraneless device efficiency at low flow rates (25 mL min⁻¹) to 60% at high flow rates (500 mL min⁻¹). The pPP membrane was significantly worse, ranging from 43% to 4% of the membraneless device efficiency at the same flow rates above. The membraneless device not only provided the highest f values, it provided reproducible f values as the device was assembled and disassembled and reassembled whereas the f values of the membrane devices varied on a daily basis and whenever a new but otherwise identical membrane was put in. The membraneless scrubber was therefore the superior device in all respects with theoretical predictions closely matching the experimental results.

The best membrane device, namely the pPTFE device was tested for all three gases: H₂S, SO₂ and NH₃. The results are shown in Fig. 6. The pPTFE device performed with uniformly lower efficiency than the membraneless device for SO₂, much like that for H₂S. However, at low flow rates it exhibited quantitative collection for NH₃, much as the membraneless device. We believe that this is due to the strong affinity of NH₃ for surfaces where water is already adsorbed. The porous membrane surface not only has water in the pores but there is adsorbed

layer of water across the membrane surface. For a gas like NH_3 , this is sufficient to provide an effective sink at lower flow rates but at higher flow rates, the difference with the membraneless device increases dramatically. For all tested gases, the amount of the analyte gas collected increases with the sampling rate but the collected fraction decreases with increasing flow rate. The net result, shown in Fig. 6a for H_2S is that the collected amount initially increases linearly with flow rate but eventually plateaus out to an essentially constant value nearly independent of the flow rate. This general behavior is true for membraneless scrubbers as well.

There are thus two flow regions advantageous for sampling – one in which the analyte gas is collected essentially quantitatively. For the membraneless scrubber, all three test gases of our interest could be collected nearly quantitatively at flow rates up to $\sim 100 \text{ mL min}^{-1}$ (experimental $f = 99.6\%$ for NH_3 , 98.8% for H_2S , and 97.3% for SO_2) and 100 mL min^{-1} is thus a desirable sampling rate for the miniature membraneless scrubber and we used this in the following experiments. Note that there is another sampling rate range around 0.5 L min^{-1} that can be useful; at this sampling rate the amount collected becomes essentially independent of the flow rate and very accurate control of the flow rate is not essential. The amount collected nevertheless will remain proportional to the analyte gas concentration. We did not further explore this strategy at this time.

Using a sampling rate of 100 mL min^{-1} , 10 min sample collection, volume make-up to 1.0 mL and subsequent analysis by flow injection as described in the experimental section, the three gases could be determined and the respective $S/N=3$ limits of detection were 1.8 ppbv for SO_2 , 1.7 ppbv for H_2S (with $5 \mu\text{M}$ FMA), and 0.29 ppbv for NH_3 . Parts per billion of these gases can be measured with relatively short (10 min) sampling time while conventional impingers require from half to a few hours gas collection.

4.3. Field application

The membraneless scrubber was used for sampling around the Mt. Aso volcanic region. The instrument package containing the membraneless scrubber as well as the pulsed fluorescence SO_2 instrument was carried to the ridge of the volcanic crater; this involved a 2-km walk through

an undeveloped trail. The pulsed fluorescence instrument monitored SO₂ continuously while the membraneless scrubber effluent was collected every 10 min. Collected samples were analyzed on the same day by ion chromatography with calibration by aqueous sulfate standard solutions (the $S/N=3$ limit of detection was 73 nM SO₄²⁻, equivalent to 1.8 ppbv SO₂ for the amount of the air sampled). The results obtained from the field experiments are shown in Fig. 7. The monitoring site was in the restricted area and we entered with a special permission for the academic purpose. High level of SO₂ was observed and sometimes it exceeded 1 ppmv in this area. Gas mask was necessary for the survey. There is excellent agreement between the two approaches. The collection device including the flow system was much easier to deploy in the field compared to the commercial instrument and our previous instrument used in volcanic gas analysis [36].

5. Conclusions

An open-channel scrubber device has been explored for the collection and analysis of gaseous atmospheric species. The collection channel was rendered hydrophilic and a thin liquid film formed thereupon to collect water soluble species effectively. The membraneless open-channel device had predictably superior gas collection efficiency compared to its membrane-interfaced counterparts and thus could provide better sensitivity or time resolution in the same analysis system. In this work, a thin cotton screen was used to obtain a hydrophilic bottom surface. Other hydrophilic surfaces inert for the purpose include anodically treated stainless steel [37], or titanium [38]; silica-treated glass [15] can also be used. An open channel miniature scrubber exhibits near-quantitative collection up to 100 mL min⁻¹ sampling rates, permits calibration with aqueous standards, allows near-exact theoretical prediction of the collection efficiency if the diffusion coefficient of the analyte gas is known and its small size facilitates field deployment. We hope to report in the near future integral systems where the analysis system has been integrated with the collector.

Newly developed spreadsheet for calculation of collection efficiency is available from the journal's website (PlanarDenuderEfficiencyCalculator.xls).

References

- [1] S. Ohira, K. Toda, *Anal. Chim. Acta* 619 (2008) 143.
- [2] K. Toda, P.K. Dasgupta, *Compr. Anal. Chem.* 54 (2008) 639.
- [3] P.K. Dasgupta, *Compr. Anal. Chem.* 37 (2002) 97.
- [4] K. Toda, *Anal. Sci.* 20 (2004) 19.
- [5] W. Whyte, G. Green, A. Albisu, *J. Aerosol Sci.* 38 (2007) 101.
- [6] K. Pant, C.T. Crowe, P. Irving, *Power Technol.* 125 (2002) 260.
- [7] G. Rosengarten, G.L. Morrison, M. Behnia, *Heat Fluid Flow* 22 (2001) 168.
- [8] D. Park, Y.-H. Kim, C.W. Park, J. Hwang, Y.-J. Kim, *J. Aerosol Sci.* 40 (2009) 415.
- [9] S. Ohira, K. Toda, *Lab Chip* 5 (2005) 1374.
- [10] K. Toda, T. Obata, V. A. Obolkin, V.L. Potemkin, K. Hirota, M. Takeuchi, S. Arita, T. Khodzher, M. Grachev, *Atmos. Environ.* 44 (2010) 2427.
- [11] K. Toda, Y. Hato, S. Ohira, T. Namihira, *Anal. Chim. Acta* 603 (2007) 60.
- [12] K. Toda, T. Koga, J. Kosuge, M. Kashiwagi, H. Oguchi, T. Arimoto, *Anal. Chem.* 81 (2009) 7031.
- [13] M. Takeuchi, J. Li, K. J. Morris and P. K. Dasgupta, *Anal. Chem.* 76 (2004) 1204.
- [14] P.K. Dasgupta, *ACS Adv. Chem. Ser.* 232 (1993) 41.
- [15] P.K. Simon, P.K. Dasgupta, Z. Vecera, *Anal. Chem.* 63 (1991) 1237.
- [16] Z. Vecera, P.K. Dasgupta, *Anal. Chem.* 63 (1991) 2210.
- [17] P.K. Simon, P.K. Dasgupta, *Anal. Chem.* 65 (1993) 1134.
- [18] C.B. Boring, S.K. Poruthoor, P.K. Dasgupta, *Talanta* 48 (1999) 675.
- [19] B. Timmer, W. Olthuis, A. v. d. Berg, *Lab Chip* 4 (2004) 252.
- [20] V. Kuban, *Crit. Rev. Anal. Chem.* 23 (1992) 323.
- [21] S. Satienerakula, S.Y. Sheikheldina, T.J. Cardwell, R.W. Cattrall, M.D. Luque de Castro, I.D. McKelvie, S.D. Kolev, *Anal. Chim. Acta* 485 (2003) 37.
- [22] N. Choengchan, P. Wilairat, P.K. Dasgupta, S. Motomizu, D.A. Nacapricha, *Anal. Chim. Acta* 579 (2006) 33.
- [23] P. Mornane, J. van den Haaka, T.J. Cardwell, R.W. Cattrall, P.K. Dasgupta, S.D. Kolev, *Talanta* 72 (2007) 741.
- [24] Z. Genfa, T. Uehara, P.K. Dasgupta, T. Clarke, W. Winiwater, *Anal. Chem.* 70 (1998) 3656.
- [25] P.G. Gormley, *Proc. Roy. Ir. Acad. A* 45 (1938) 59.
- [26] P.G. Gormley, M. Kennedy, *Proc. Roy. Ir. Acad. A* 52 (1949) 163.
- [27] P.A. McCuen, Heat transfer with laminar and turbulent flow between parallel planes with constant and variable wall temperature and heat flux. Ph.D. Dissertation, Stanford University, 1961.
- [28] R.E. Lundberg, W.C. Reynolds, W.M. Kays, 1963. NASA Technical Note D-1972, National Aeronautics and Space Administration: Washington D.C.
- [29] J.M. Berg, D.L. James, C.F. Berg, K. Toda, P.K. Dasgupta, *Anal. Chim. Acta* 664 (2010) 56.
- [30] K. Toda, P.K. Dasgupta, J. Li, G.A. Tarver, G.M. Zarus, *Anal. Chem.* 73 (2001) 5716.
- [31] Z. Genfa, P.K. Dasgupta, *Anal. Chem.* 61 (1989) 408.
- [32] S. Ohira, K. Toda, *J. Chromatogr. A* 1121 (2006) 280.
- [33] S. Fujita, *Kagaku Kogaku* 28 (1964) 251 – 254.
- [34] *Kagaku Kogaku Binran*, 4th ed.: Kagaku Kyokai Ed.; Maruzen: Tokyo, 1978; pp.66 – 69.
- [35] McKays, W.; Crawford, M. E. *Covective heat and mass transfer*. 2nd ed., McGraw-Hill, 1980

pp. 66-68.

[36] K. Toda, S. Ohira, T. Tanaka, T. Nishimura, P.K. Dasgupta, *Environ. Sci. Technol.* 38 (2004) 1529.

[37] K. Toda, J. Li, P.K. Dasgupta, *Anal. Chem.* 78 (2006) 7284.

[38] J. Premkumar, *Chem. Mater.* 17 (2005) 944.

Figure captions

Fig. 1. Diffusion of gas molecules in a planar open channel. Decrease of gas concentration is shown as gradation. See text for details.

Figure 2. Structure of the planar open channel scrubber. In the left, only channels for solution and air are drawn to simplify the figure and they are attached to a bottom plate and a top plate, respectively. Actual membrane device and membraneless device were shown back side and front side, respectively, in the picture. A membrane (shown in dotted outline) was used only in selected comparison experiments. Dimensions are all expressed in mm.

Fig. 3. Experimental and computed collection efficiency vs. sampling rate for NH_3 , H_2S and SO_2 . The lines (solid, dashed and dotted) respectively depict the theoretical curves for the three gases. Gas channel depth: 1.5 mm.

Fig. 4. Effect of gas channel height. Symbols and lines respectively depict experimental data and theoretical estimates. Test gas: H_2S .

Fig. 5. Collection efficiencies of membrane scrubbers utilizing three different membrane types compared to a membraneless device of identical dimensions. Test gas 1 ppmv H_2S , 1.5-mm gas channel depth. For the silicone membrane, 100 ppmv H_2S had to be used to make the measurement of the collected analyte possible.

Fig. 6. Collection efficiency obtained with the membraneless (●) and pPTFE (●) devices for 1 ppmv H_2S (a), 1 ppmv SO_2 (b) and 100 ppmv NH_3 gases (c). Open circles ○ shown in panel (a) are the experimental amounts of H_2S collected (in nmol) and the dashed line indicates the total amount of H_2S sampled.

Fig. 7. Field data obtained around Mt. Aso Volcano, September 1, 2009. Thick horizontal lines are

SO₂ level obtained from membraneless scrubber collection and subsequent ion chromatography analysis. Solid (blue) continuous trace and the horizontal dashed lines are raw signals obtained by the commercial UV-fluorescence instrument and its 10-min averages, respectively.

Figure 1

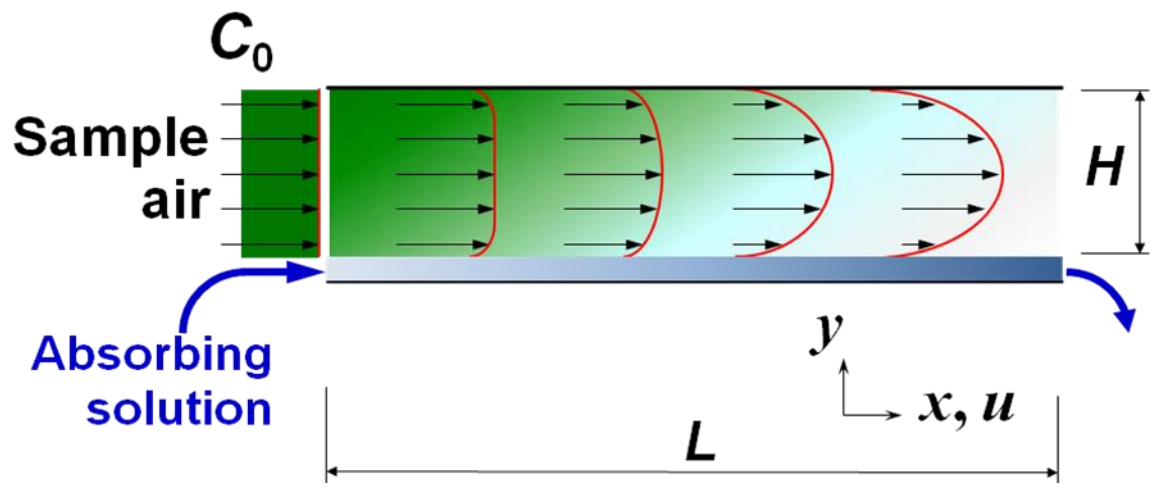


Figure 2

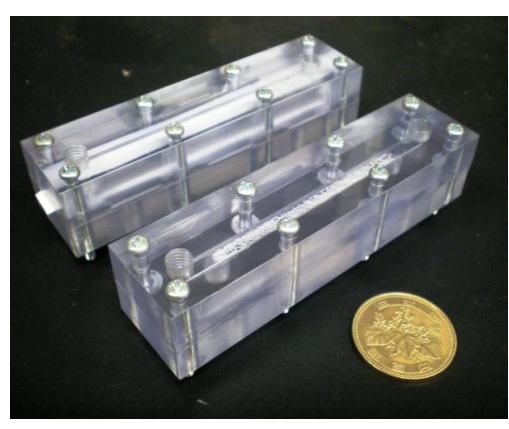
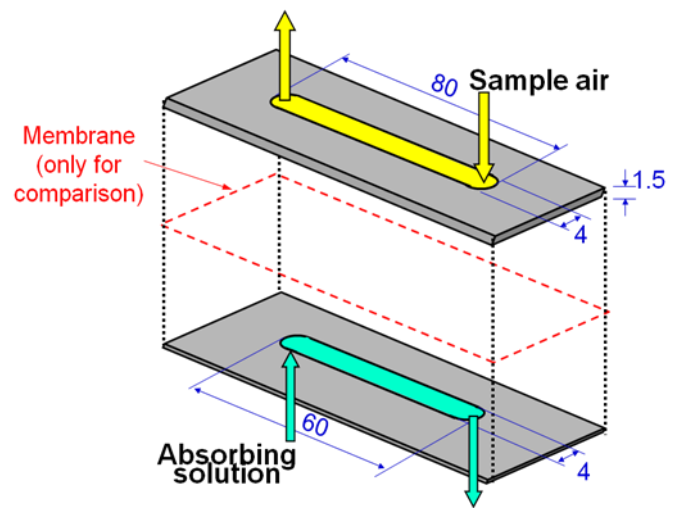


Figure 3

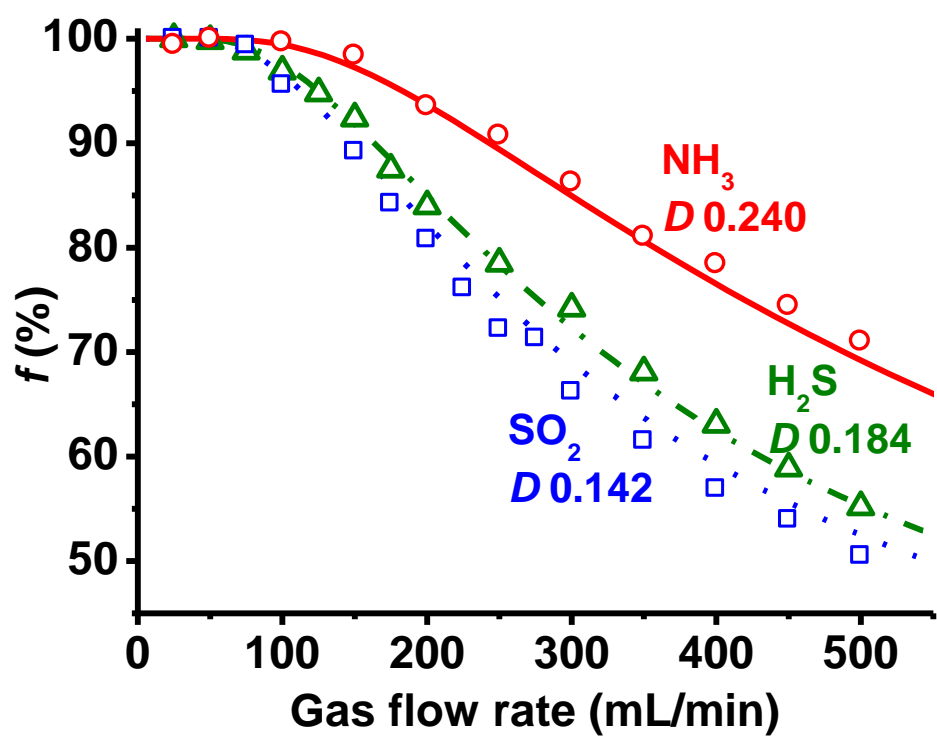


Figure 4

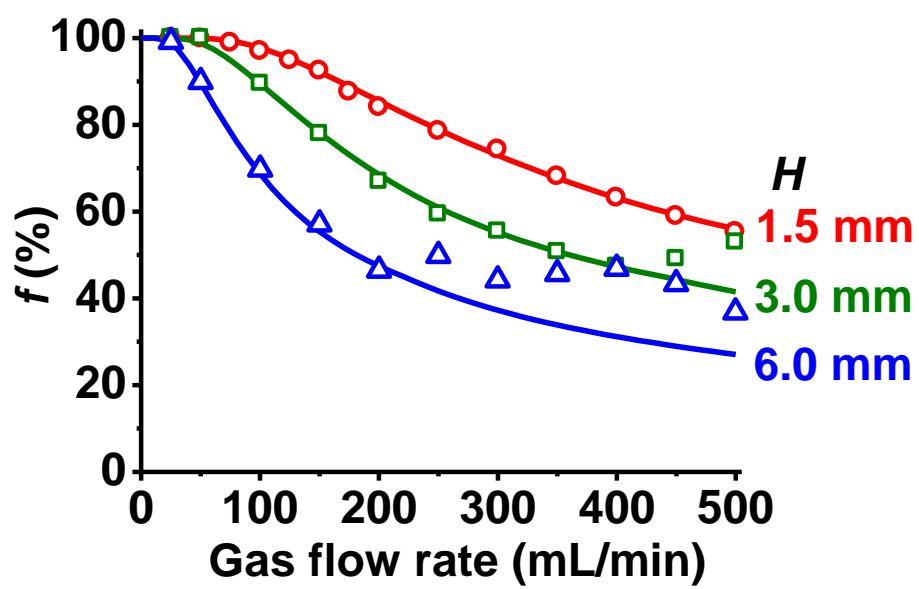


Figure 5

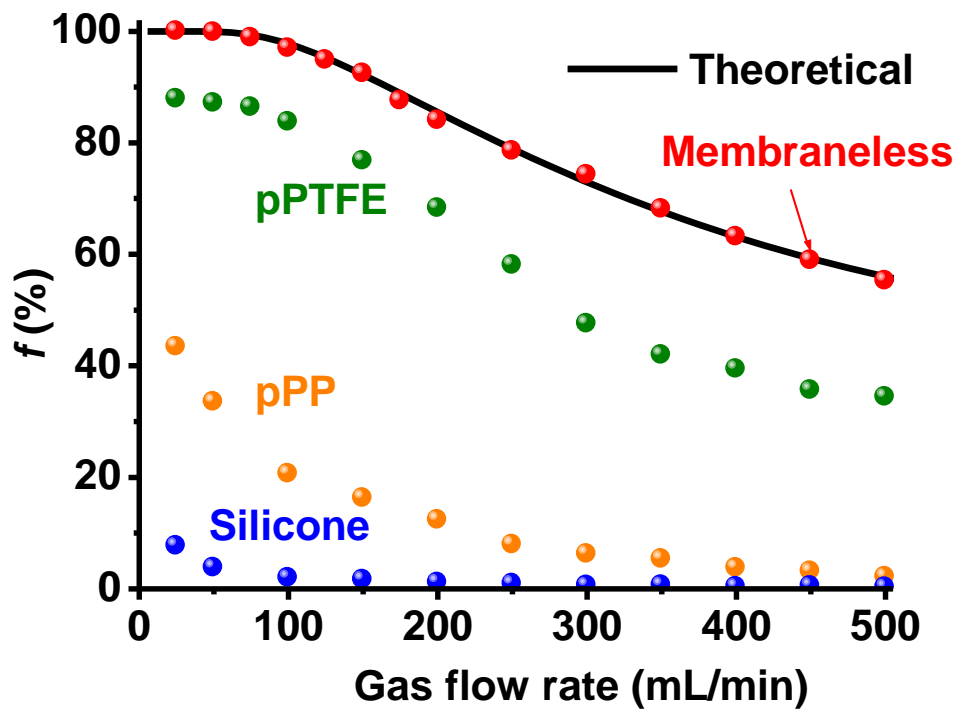


Figure 6

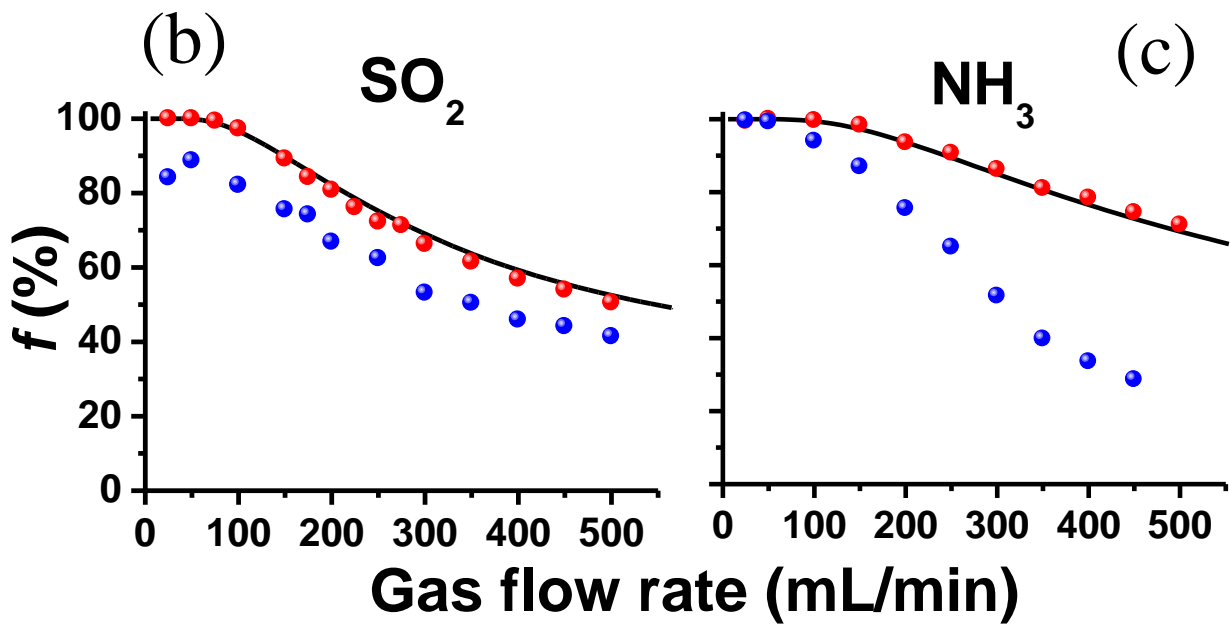
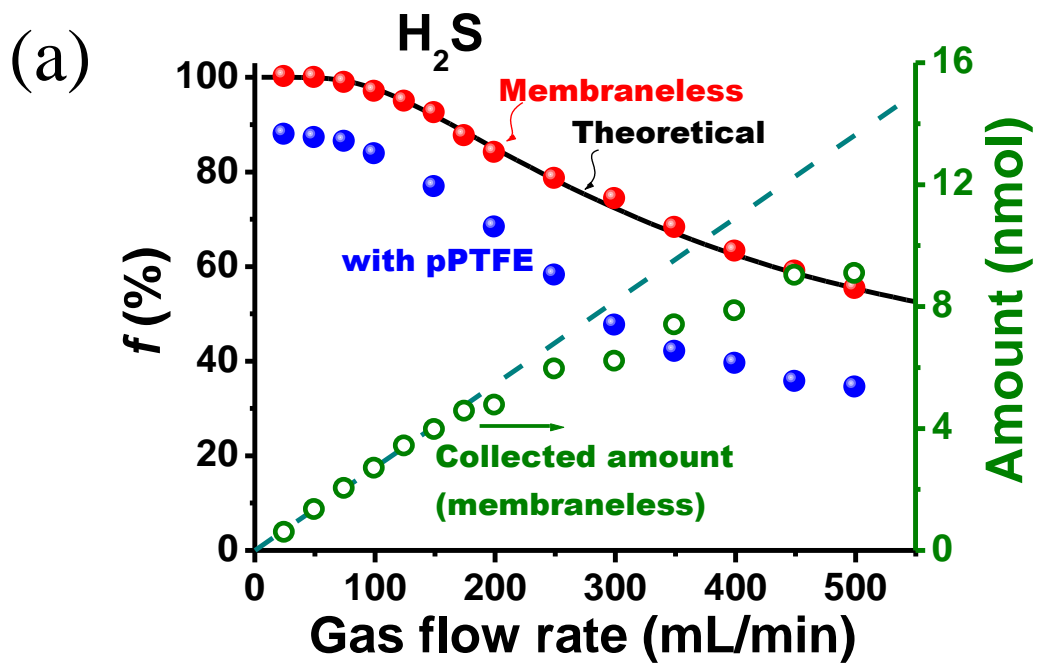
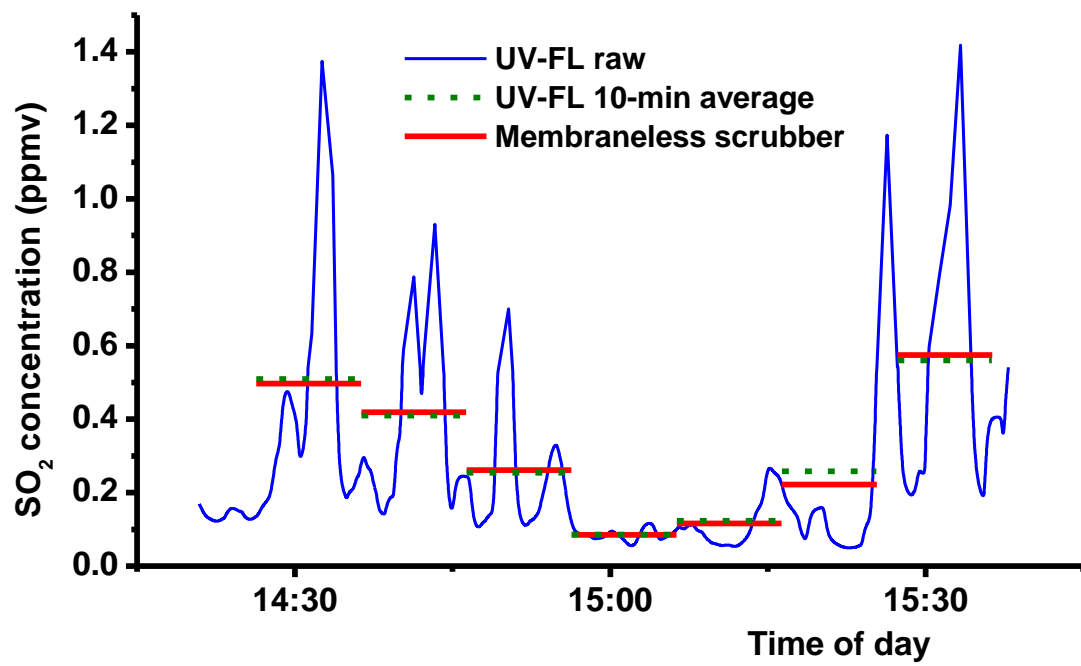


Figure 7



Length (cm)	h (cm)	w (cm)	Vol Flow (cm ³ /min)	Flow Units	Flow Rate
6	0.15	0.4	8.3335	liter/min	0.5
			Vol Flow (l/min)		
			0.5		

x type	x Plot Start (cm)	x Num	Q type	Qi (cm ³ /sec)	Qf (cm ³ /sec)
linear	0.00E+00	80	linear	0.16667	8.3335
		x Inc			
		0.075			

Re*Sc Hydraulic Dia Velocity (cm/s)
 226.453804 0.3 138.891667

Last 5 Points	
x (cm)	f
6	0.60928566
5.925	0.60516844
5.85	0.60102318
5.775	0.59684968
5.7	0.59264777

xBar Points	Fit Method
0	power
0.0001	power
0.001	power
0.0025	power
0.005	power
0.01	power
0.025	expon
0.05	expon
0.1	expon
0.25	expon
1.00E+10	n/a

Full Length		
x (cm)	f	
0		0
0.075	0.03820047	
0.15	0.06074183	
0.225	0.07754584	
0.3	0.0914373	
0.375	0.10548357	
0.45	0.12043632	
0.525	0.13472075	
0.6	0.14845692	
0.675	0.16173106	
0.75	0.17307472	
0.825	0.18395014	
0.9	0.19447426	
0.975	0.20468641	
1.05	0.21461887	
1.125	0.22429851	
1.2	0.23374803	
1.275	0.2429868	

Varying Q			
Q (cm ³ /s)	f	Q (liter/min)	
0.16667		1	0.0100002
0.5750115	0.99999711		0.03450069
0.983353	0.99943796		0.05900118
1.3916945	0.99503873		0.08350167
1.800036	0.98369594		0.10800216
2.2083775	0.9654923		0.13250265
2.616719	0.94220243		0.15700314
3.0250605	0.91577693		0.18150363
3.433402	0.88778352		0.20600412
3.8417435	0.85933399		0.23050461
4.250085	0.83116408		0.2550051
4.6584265	0.80373518		0.27950559
5.066768	0.77731947		0.30400608
5.4751095	0.75206265		0.32850657
5.883451	0.7280276		0.35300706
6.2917925	0.70522414		0.37750755
6.700134	0.68362887		0.40200804
7.1084755	0.66319842		0.42650853